Journal of Chromatography A, 1218 (2011) 4619–4626

Contents lists available at ScienceDirect

Journal of Chromatography A

journal homepage: www.elsevier.com/locate/chroma

Development of magnetic multiwalled carbon nanotubes combined with near-infrared radiation-assisted desorption for the determination of tissue distribution of doxorubicin liposome injects in rats

Shun Shen[a,b,1], Jinfeng Ren[a,b,1], Jun Chen[a,b], Xiaohui Lu[c], Chunhui Deng[c], Xinguo Jiang[a,b,*]

[a] School of Pharmacy, Fudan University, No. 826 Zhangheng Road, Shanghai 201203,China
[b] Key Laboratory of Smart Drug Delivery, Ministry of Education & PLA, China
[c] Department of Chemistry, Fudan University, No.220, Handan Road, Shanghai 200433,China

ARTICLE INFO

Article history:
Received 31 January 2011
Received in revised form 13 May 2011
Accepted 17 May 2011
Available online 27 May 2011

Keywords:
Magnetic multiwalled carbon nanotubes
Near-infrared radiation-assisted desorption
Doxorubicin
Rat tissue

ABSTRACT

For the first time, magnetic multiwalled carbon nanotubes (MWNTs) combined with near-infrared radiation-assisted desorption (NIRAD) was successfully developed for the determination of tissue distribution of doxorubicin liposome injects (DOXLI) in rats. The magnetic MWNTs nanomaterials were synthesized via a simple hydrothermal process. Magnetic Fe_3O_4 beads, with average diameters of *ca.* 200 nm and narrow size distribution, were decorated along MWNTs to form octopus-like nanostructures. The hybrid nanocomposites provided an efficient way for the extraction and enrichment of doxorubicin (DOX) via π–π stacking of DOX molecules onto the polyaromatic surface of MWNTs. DOX adsorbed with magnetic MWNTs could be simply and rapidly isolated through a magnetic field. In addition, due to the near-infrared radiation (NIR) absorption property of MWNTs, irradiation with NIR laser was employed to induce photothermal conversion, which could trigger rapid DOX desorption from DOX-loaded magnetic MWNTs. Extraction conditions such as amount of magnetic MWNTs added, pH values, adsorption time, desorption solvent and NIR time were investigated and optimized. Method validations including linear range, detection limit, precision, and recovery were also studied. The results showed that the proposed method based on magnetic MWNTs coupled to NIRAD was a simple, rapid and high efficient approach for the analysis of DOXLI in rat tissues.

1. Introduction

Carbon nanotubes (CNTs) have been intensively explored for biological and biomedical applications in the past few years due to their unique physical and chemical properties [1–10]. CNTs can be classified into two groups: single-walled carbon nanotubes (SWNTs) and multiwalled carbon nanotubes (MWNTs) based on the principle of the hybridized carbon atom in the walls of CNTs. In particular, MWNTs have become the most attractive carbon nanostructure sorbent materials in analytical processes [11–22] because of their extremely large surface areas. MWNTs allow efficient loading of multiple molecules alongside the nanotube wall. Aromatic molecules can be easily bound onto the polyaromatic surface of nanotubes through supramolecular π–π stacking interactions. Thus, MWNTs adsorbent outperformed many popular solid-phase extractants and was successfully applied to preconcentration, extraction and sorption of organic and inorganic pollutants in water [23,24], polybrominated diphenyl ethers in milk [25], barbiturates and benzodiazepines in pork [26]. However, as the sample extraction materials, MWNTs are not easy to isolate, and tedious centrifugation steps are often required for further separation. In addition, the uncontrolled release of MWNTs into the environment is of concern because of their nanoscale particle sizes. They can penetrate into cells, causing damage to plants, animals, and humans. The toxicology was highlighted recently [27]. The above disadvantages would limit their broad analytical applications.

Recently, magnetic manipulation techniques have become more and more popular since they are simple, rapid, low cost and highly efficient. Magnetic nanoparticles (MNPs), mainly including Fe_3O_4 NPs, are of great interest to researchers. MNPs adsorbed with target components can be easily collected by an external magnetic field. Hence, MNPs have been developed for extraction and enrichment of cells [28], proteins [29], peptides [30], ergosterol [31], polycyclic aromatic hydrocarbons [32], perfluorinated compounds [33], methylprednisolone [34] and so on.

* Corresponding author at: School of Pharmacy, Fudan University, No. 826 Zhangheng Road, Shanghai 201203, China. Tel.: +86 21 51980067; fax: +86 21 51980069.
E-mail address: xgjiang@shmu.edu.cn (X. Jiang).
[1] These two are the first authors having given equal contribution.

0021-9673/$ – see front matter © 2011 Elsevier B.V. All rights reserved.
doi:10.1016/j.chroma.2011.05.060

Clever combinations of MWNTs with MNPs will benefit their further development, which appears as an interesting advanced composite material as a result of their strong sorption and superparamagnetic properties. The multifunctional nanocomposites could facilitate the separation and recovery of the solid material from the solution by an externally applied magnetic field after extraction and enrichment. Lately, Morales-Cid et al. [35] applied magnetic MWNTs to preconcentrate (fluoro)quinolones in human plasma. The results showed that the enrichment ability of magnetic MWNTs was highly effective and sample preparation manipulation was simplified by the above method.

Herein, we developed magnetic MWNTs for enrichment and separation of cancer chemotherapy drug of DOX to study tissue distribution of DOXLI in rats. DOX could retain high affinity with CNTs from noncovalent π–π stacking, and numerous papers have reported the use of CNTs as DOX delivery vehicles for cancer therapies [3,8]. However, the release behavior of DOX from CNTs depends on the pH of a solution. Even in the most suitable release condition (pH 4–5 PBS solution), only 40% DOX was released within 1 day according to the report [3,8]. Obviously, this result cannot satisfy the drug analysis for the rapid and accurate requirements. Therefore, developing a rapid and efficient extraction method is of great interest. Fortunately, CNTs have the unique physical property that can absorb NIR radiation to induce substantial vibration energy, which produces localized heating. The extraordinary photon-to-thermal energy conversion can significantly increase the DOX release amount from CNTs [8]. To our best knowledge, for the first time, we developed a novel method based on magnetic MWNTs combined with near-infrared radiation-assisted desorption (NIRAD) for rapid and simple analysis of DOXLI from rat tissues. Extraction and desorption conditions were optimized. To demonstrate the validation of the proposed method, the quantification limit, linearity and precision were investigated.

2. Materials and methods

2.1. Material and chemicals

The standards of doxorubicin hydrochloride, daunorubicin hydrochloride (internal standard, I.S.), methanol and acetonitrile (ACN), n-hexane, isopropanol, ethyl acetate and chloroform (HPLC grade) were purchased from Sigma–Aldrich Chemical Company (St. Louis, MO, USA). Iron chloride hexahydrate ($FeCl_3{\cdot}6H_2O$), ethylene glycol (EG) and poly(ethylene glycol)-20000 (PEG-20000) were purchased from Aladdin reagent, Inc. (Shanghai, China). MWNTs with 5–15 μm in length and 20–40 nm in diameter (95% purity in MWNTs) were obtained from Shenzhen Nanotech Port Co., Ltd. (Shenzhen, China). The other reagents were analytical grade and acquired from Sinopharm Chemical Reagent Co., Ltd. (Shanghai, China). Ultrasonic cell disrupter system (Branson, S-250D) was purchased from High Quality Instrument Co., Ltd. (Shanghai, China). All aqueous solutions were prepared using Milli-Q water by Milli-Q system (Millipore, Bedford, MA, USA).

Doxorubicin hydrochloride liposome injects (commercial name, Caelyx) were acquired from Ben Venue Laboratories, Inc. (State of Tennessee, USA). Standard stock solution of the target analyte was prepared by dissolving the required amounts in phosphate buffered saline (PBS) solutions to obtain a concentration of 200 μg/mL, and subsequently stored at 4 °C.

Various types of tissues including hearts, livers, spleen, lungs and kidneys were harvested, put into saline solution to remove the blood or content, blotted with the filter paper, and then stored at −20 °C.

2.2. Preparation of magnetic MWNTs

The magnetic MWNTs were prepared according to the previous method [36,37] as shown in Fig. 1a. Firstly, the pristine MWNTs were dispersed into concentrated nitric acid at 140 °C with refluxing for 8 h. Then, the black solution was treated with ultrasonicator for 30 min. Afterwards, the solution was diluted with distilled water and rinsed several times until the pH value reaches neutral. The resulting MWNTs were separated from the solution by filtration and dried in vacuum at 60 °C for further use.

Secondly, the generation of magnetic Fe_3O_4 beads was carried out by reduction reactions between $FeCl_3$ and ethylene glycol in the hydrothermal system as described in Refs. [23,24]. Typically, 0.81 g (3 mmol) $FeCl_3{\cdot}6H_2O$ was dissolved into 40 mL ethylene glycol to form an orange solution. Then, 200 mg acid-treated MWNTs were dispersed in the solution by ultrasonication for 3 h. After that, 0.15 g trisodium citrate, 3.6 g NaAc and 1.0 g PEG-20000 were added with constant stirring for 30 min. The mixture was sealed in a Teflon-lined stainless steel autoclave, maintained at 200 °C for 8 h, and then cooled to ambient temperature. The black products were finally rinsed with ethanol several times and dried at 60 °C for 10 h.

2.3. Apparatus and measurement

Scanning electronic microscope (SEM) images were recorded on a Philips XL30 electron microscope (Netherlands) operating at 20 kV. Transmission electron microscopy (TEM) images were obtained using a JEOL JEM-2010 microscope (Japan) operated at 200 kV. Powder X-ray diffraction (XRD) patterns were recorded on a Bruker D4 X-ray diffractometer with Ni-filtered Cu K_R radiation (40 kV, 40 mA). The Raman spectra were recorded at room temperature on a LabRam-1B Raman spectrometer with a laser at an excitation wavelength of 632.8 nm. The magnetic properties of the magnetic MWNTs were measured using a superconducting quantum interference device (SQUID) at room temperature.

Ultrasonics Corporation (Danbury, USA) and the 808-nm continuous-wave NIR laser were from Changchun New Industries Optoelectronics Technology (Changchun, China). HPLC was performed with a Shimadzu (Kyoto, Japan) system comprising an LC-10AT VP pump, an RF-10A XL fluorescence detector, and a CTO-10 AS VP column oven. Empire HS-2000 software was used for data acquisition. The chromatographic separation of DOX from rat tissues was performed on a Hypersil BDS silica C_{18} (5 μm, 4.6 mm × 200 mm) at 25 °C. The mobile phase, delivered at 1.2 mL/min under isocratic conditions, consisted of KH_2PO_4 (0.01 mol/L)–ACN–water (145:55:0.6, v/v). The excitation wavelength was set at 480 nm, while the emission wavelength was set at 550 nm. The injection volume was 10 μL.

2.4. Investigation of magnetic MWNTs extraction conditions

Extraction conditions such as amount of magnetic MWNTs added, pH conditions, adsorption time, desorption solvents and NIR illumination time were investigated.

10 μL of DOX and I.S. (200 μg/mL), together with 50, 100 and 150 μL of magnetic MWNTs (1 mg/mL), respectively, were diluted to 300 μL by PBS solution at the range of pH values from 4 to 10. The mixed solutions were continuously ultrasonicated (200 W, 59 kHz) with different time from 1 to 15 min in ice bath. Finally, the captured DOX-magnetic MWNTs were isolated by placing an Nd–Fe–B magnet in the bottom of EP tube and the residue solution was analyzed

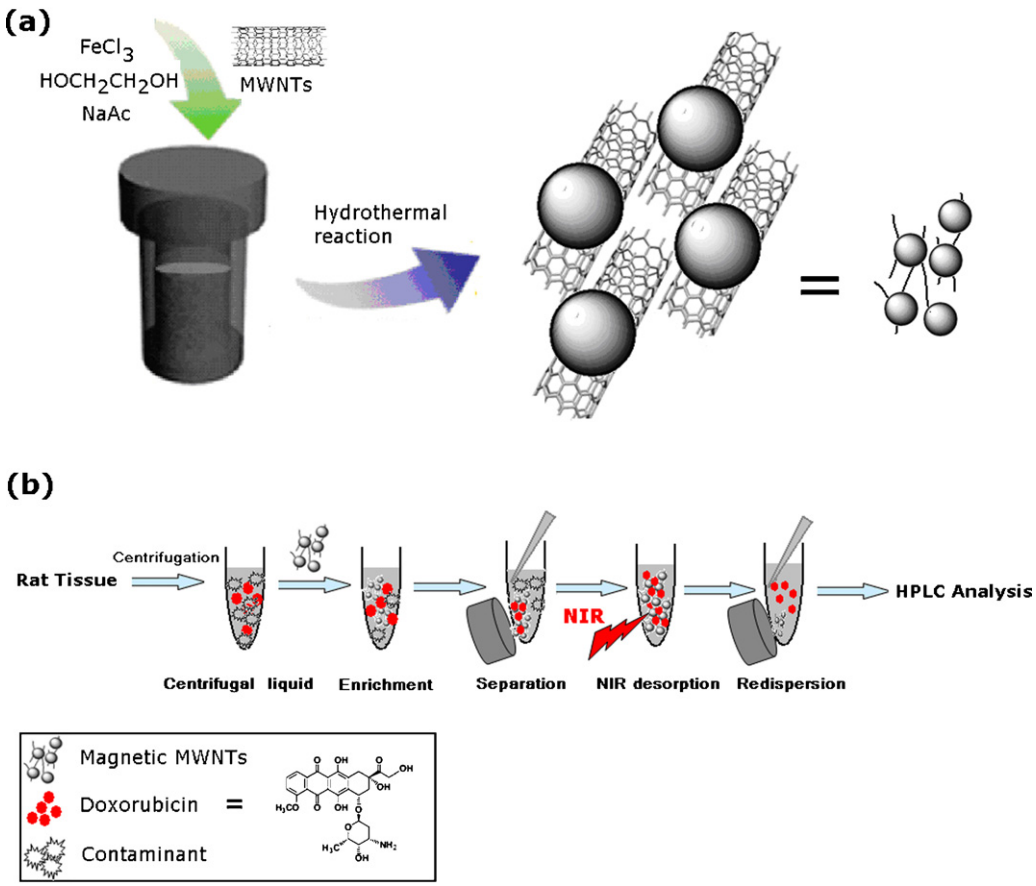

Fig. 1. Synthesis procedure (a) and extraction process of DOX in centrifugal liquid of rat tissues (b) of magnetic MWNTs nanomaterials.

by HPLC to optimize the adsorption conditions. The adsorption ratio of DOX (%) was calculated by Eq. (1).

$$\text{The adsorption ratio of DOX (\%)} = \frac{100\% \times (\text{Peak area of DOX in origin solution} - \text{Peak area of DOX in residue solution})}{\text{Peak area of DOX in origin solution}} \quad (1)$$

Subsequently, the conditions of desorption solvents and NIR duration, were also investigated. The captured DOX absorbed with magnetic MWNTs was rinsed by different organic solvents, including methanol, ACN, n-hexane, isopropanol, ethyl acetate and chloroform and the mixture of pH 3.5 PBS and methanol. In order to accelerate DOX extraction efficiency, NIR were also employed to study the desorption effects.

2.5. Linear range, detection limit, precision, and recovery

Different amounts of DOX and 10 μL of I.S. (200 μg/mL) were added to 50 mg of drug-free tissue samples to a final concentration of DOX at 0.005, 0.025, 0.05, 0.25, 0.5 and 1.25 μg/50 mg. Then, 500 μL of PBS solution (pH 3.5) was added. After homogenized by an ultrasonic cell homogenizer in ice bath for 15 s, the sample was allowed to stand for 2 h at 37 °C. Then, 200 μL supernatant was removed after centrifugation and its pH was adjusted to 9.2. The calibration curve was obtained by plotting the peak area ratio between DOX and I.S. using optimal magnetic MWNTs conditions.

Detection limit (DL) was determined by five analyses of the lowest concentration in spiked drug-free tissues (2 ng/50 mg tissues). DL was calculated on the basis of extrapolation to a signal-to noise ratio of 3.

The intra- and inter-run precision and accuracy of the assay were determined by five replicate analyses of the DOX concentration in drug-free tissues (0.005, 0.05 and 1.25 μg/50 mg) plus I.S solution within day and on continuous 5 days. The obtained peak areas were used for the calculation of the relative standard deviations (RSDs).

Recoveries were carried out by adding 0.005, 0.05 and 1.25 μg DOX to the 50 mg rat tissues containing known content of DOX. Triplicate measurements were performed.

2.6. Determination of DOX in rat samples using the magnetic MWNTs

Normal male Kunming rats were purchased from Institute of Laboratory Animal Science (Beijing, China). One day prior to the study, the rats were subjected to right external jugular vein catheter under ketamine/xylazine anesthesia. Cannula patency was maintained using heparinized saline (42 U heparin/mL saline). After 24 h of recovery from the surgery, forty-eight rats were given 5 mg kg^{-1} DOXLI via the jugular vein catheter. The tissues including hearts, livers, spleen, lungs and kidneys were harvested at 1, 4, 12, 24, 48, 72, 120 and 168 h (n = 6 at each time point), then put into saline solution to remove the blood or content, blotted on filter paper, and finally stored at −20 °C. The route for the extraction of DOX is shown in Fig. 1b and the

sample was analyzed as described under the optimized conditions.

3. Results and discussion

3.1. Preparation and characterization of the magnetic MWNTs nanocomposites

The synthetic protocol of magnetic MWNTs is presented in Fig. 1a. Magnetic Fe_3O_4 spheres were decorated along HNO_3-pretreated MWNTs via a solvothermal reaction according to a previous report [36,37]. The size and morphology of the as-produced sample were investigated by transmission electron microscopy (TEM). A representative TEM image (see Supplementary material, Fig. S1a) of the obtained magnetic MWNTs revealed that the MWNTs were decorated with the spherical particle with a diameter of about 200 nm. The nanostructure appeared like octopus with abundant MWNTs. The scanning electron microscopy (SEM) image (Fig. S1b) of the magnetic MWNTs indicated that the product consisted of a large quantity of spherical nanobeads and carbon nanotubes.

The wide angle XRD pattern (Fig. S2) indicated that the crystal structure of magnetic nanocomposites comprised two phases of cubic Fe_3O_4 (JCPDS file No. 190629) and CNTs. Well-resolved diffraction peaks revealed the good crystallinity of the Fe_3O_4 specimens, locating at 2θ of 30.28°, 35.56°, 43.3°, 53.68°, 57.36°, 62.72°, 74.04° and 74.68°, respectively. These data matched well with the peer Refs. [38,39]. The diffraction peak at $2\theta = 26.4°$ was the typical Bragg peak of pristine CNTs and could be indexed to the (0 0 2) reflection of CNTs. Without extra diffraction peaks in the spectrum, it was concluded that the third phase did not exist. Raman spectroscopy has been extensively used to probe the structural and electronic properties of CNTs. The Raman spectra of MWNTs (Fig. S3a) showed the higher intensity of D bands (1336 cm^{-1}) in comparison to G bands (1585 cm^{-1}), which was due to the presence of more defects at the surface of MWNTs. A small shift in G band and D band peaks was observed in the case of magnetic nanocomposite (Fig. S3b). Along with a shift in G and D bands, the characteristic band centered at 668 cm^{-1} was observed at lower Raman shift values in the magnetic MWNTs. This band indicated that the magnetic Fe_3O_4 nanoparticles were successfully immobilized on the surface of MWNTs.

Magnetic characterization was carried out by magnetometry at 300 K using a superconducting quantum interference device (SQUID). The magnetization value was measured to be 31.09 emu g^{-1} for magnetic MWNTs. Fig. 2a indicated the superparamagnetic properties of magnetic MWNTs with its hysteresis loop due to the presence of nanometer-sized magnetite particles. Meanwhile, the magnetic MWNTs in their homogeneous dispersion (Fig. 2b) showed fast moment to the applied magnetic field (Fig. 2c) and redispersed quickly with a slight shake once the magnetic field was removed. It demonstrated that the magnetic MWNTs possessed excellent magnetic responsivity and redispersibility, which is an advantage to its further applications.

3.2. Adsorption of DOX onto magnetic MWNTs

DOX, a commonly used cancer chemotherapy drug, is most probably adsorbed on the surface of CNTs with strong loading capacity and not absorbed into. Many studies have been reported that the amount of DOX bound onto CNTs was pH dependent [3,8]. The pH of the solution has a critical effect on analyte-magnetic MWNTs interactions. Thus, different pH conditions from 4 to 10 were investigated with 150 μL magnetic MWNTs (1 mg/mL) as described in Section 2.4 under the optimized conditions. After

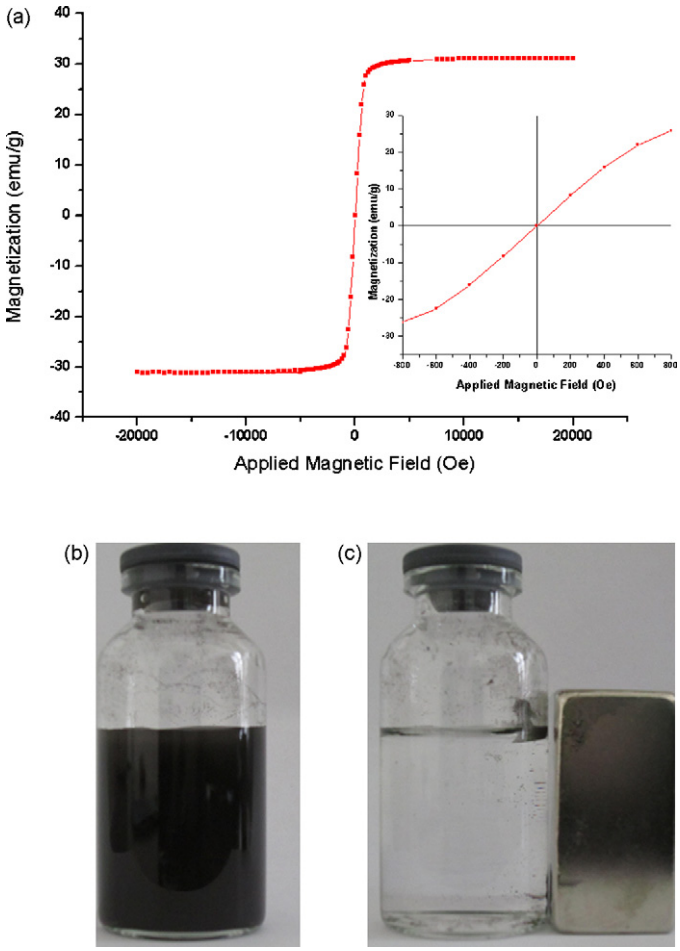

Fig. 2. (a) The magnetic hysteresis loops of the magnetic MWNTs recorded at 25 °C. (b) The photos of the aqueous dispersion of the magnetic MWNTs before and (c) after separation with a magnet for a few seconds, indicating a fast separation process of the microspheres in the dispersion.

extraction was performed by magnetic MWNTs with ultrasonication for 5 min, the drug-magnetic MWNTs were separated by placing a permanent magnet made of Nd–Fe–B and the residue solution was analyzed by HPLC. As shown in Fig. 3a, the best absorption efficiency for DOX was achieved at pH 9.2. The obtained results were consistent with those reported and showed that our as-prepared magnetic MWNTs could be used as sorbents to enrich DOX effectively in weak alkaline solution.

The amount of sorbent added is known to be correlated with the quantity of analyte adsorbed. Thus, the optimization of the magnetic MWNTs nanomaterials added amounts was performed. The experiment condition was the same as mentioned above. Fig. 3b indicated that the highest enrichment efficiency for DOX (2 μg) achieved at the addition amount of 150 μg of magnetic MWNTs.

Extending contact time facilitates analyte–particle interaction until equilibrium is reached. Additionally, sonication helps to disperse the magnetic MWNTs, and increase the contact area between magnetic MWNTs and DOX, which can accelerate the adsorption [34]. The above-described optimal conditions were conducted to investigate the adsorption kinetics of DOX on magnetic MWNTs. As shown in Fig. 3c, the adsorption amount for DOX increased significantly when extraction time rose from 1 to 5 min under continuous sonication. Once adjusted from 5 to 15 min, the adsorption amounts had no remarkable increase. Meanwhile, the DOX adsorption amount without sonication was significantly less than that with sonication.

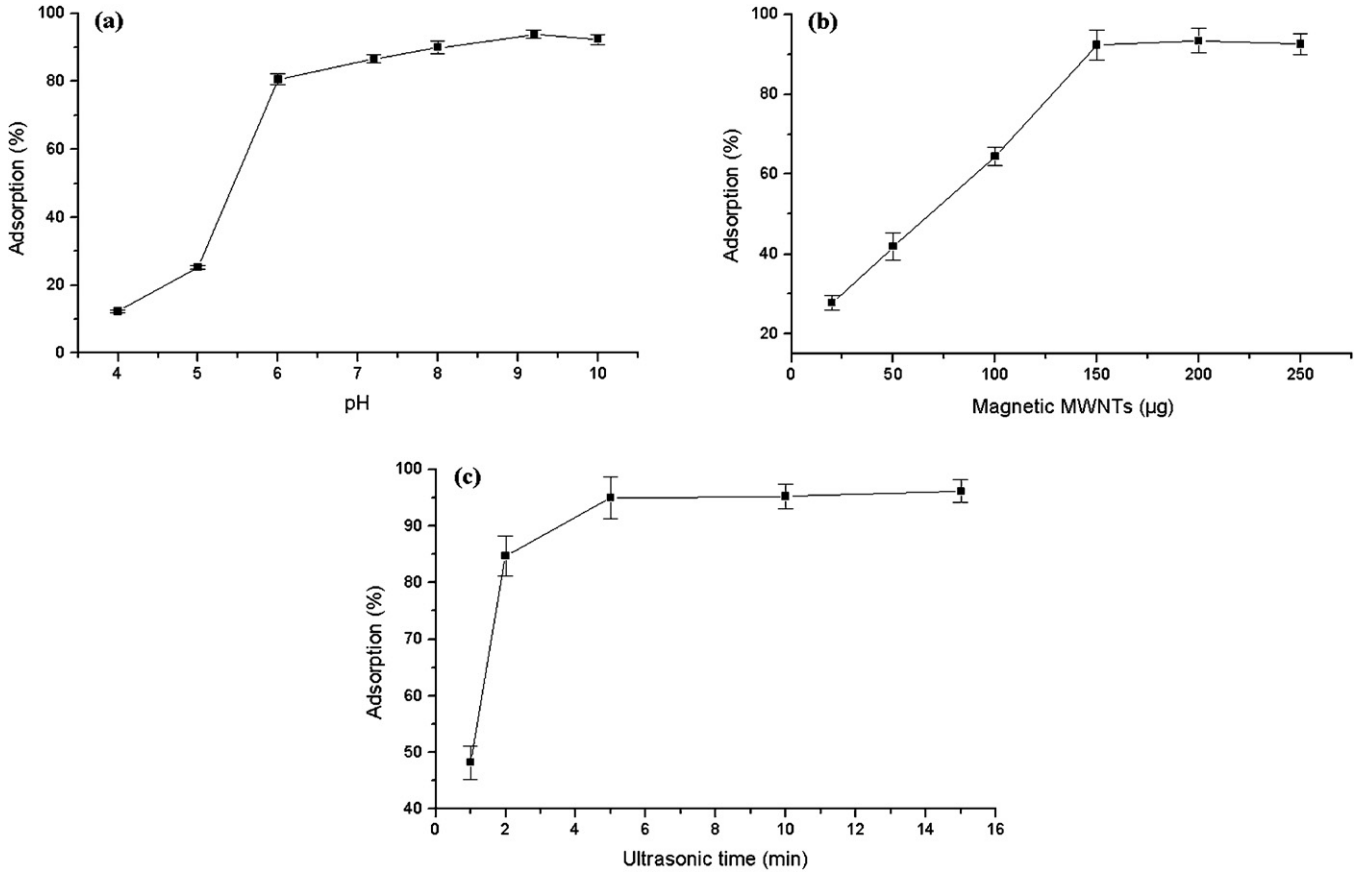

Fig. 3. The effect of (a) pH on the adsorption of DOX to magnetic MWNTs, (b) magnetic MWNTs amount added on the adsorption of DOX to magnetic MWNTs and (c) contact time on the adsorption of DOX to magnetic MWNTs with sonication in ice bath ($n = 3$ for each point).

Therefore, the optimized conditions including pH 9.2 solution, 150 μL of magnetic MWNTs (1 mg/mL) added, contact time of 5 min with continuous ultrasonication were selected for further study.

3.3. Desorption of DOX from magnetic MWNTs

Firstly, organic solvent elution approaches were attempted to elute DOX from magnetic MWNTs because the elution of absorbed analytes was much easier than that of physically adsorbed analytes on the surface of the MWNTs owing to the π–π interaction between the aromatic ring(s) of the target analytes and the MWNTs. Various organic solvents including methanol, ACN, n-hexane, isopropanol, ethyl acetate and chloroform was adopted to investigate the desorption effects. As shown in Table 1, the DOX recovery of 70.1% was obtained by the mixture of chloroform/methanol (4:1, v/v). However, the result was unsatisfactory. Moreover, the use of organic solvents can cause harm to the human body and the mixture of chloroform/methanol was not suitable for direct injection analysis by HPLC.

As we know, DOX release from CNTs is also pH dependent. In acidic PBS solutions, the release amount is higher than that in alkaline medium. Thus, PBS solutions of pH 3.5 mixed with different ratio of methanol were also explored. As shown in Table 1, the recoveries of DOX keep increasing with the rise of methanol

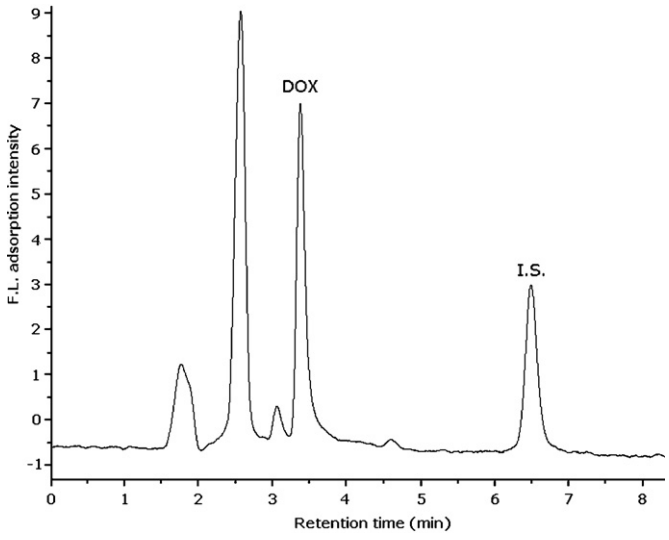

Fig. 4. The representative chromatograms of rat heart tissue after the injection of a single 5 mg kg^{-1} dose of DOXLI.

Table 1
The recovery of different eluents to release DOX from magnetic MWNTs ($n = 3$).

Eluent	Recoveries (%)
Methanol	35.5 ± 2.1
Acetonitrile	19.6 ± 1.5
Hexane	3.9 ± 3.7
Isopropanol	12.0 ± 2.2
Ethyl acetate	34.4 ± 3.9
Chloroform	9.3 ± 4.1
Chloroform:methanol (1:1, v/v)	62.2 ± 3.8
Chloroform:methanol (4:1, v/v)	70.1 ± 1.2
pH 3.5 PBS	51.6 ± 0.9
pH 3.5 PBS:methanol (3:1, v/v)	59.4 ± 1.6
pH 3.5 PBS:methanol (1:1, v/v)	63.4 ± 2.1
pH 3.5 PBS:methanol (1:3, v/v)	71.2 ± 1.6

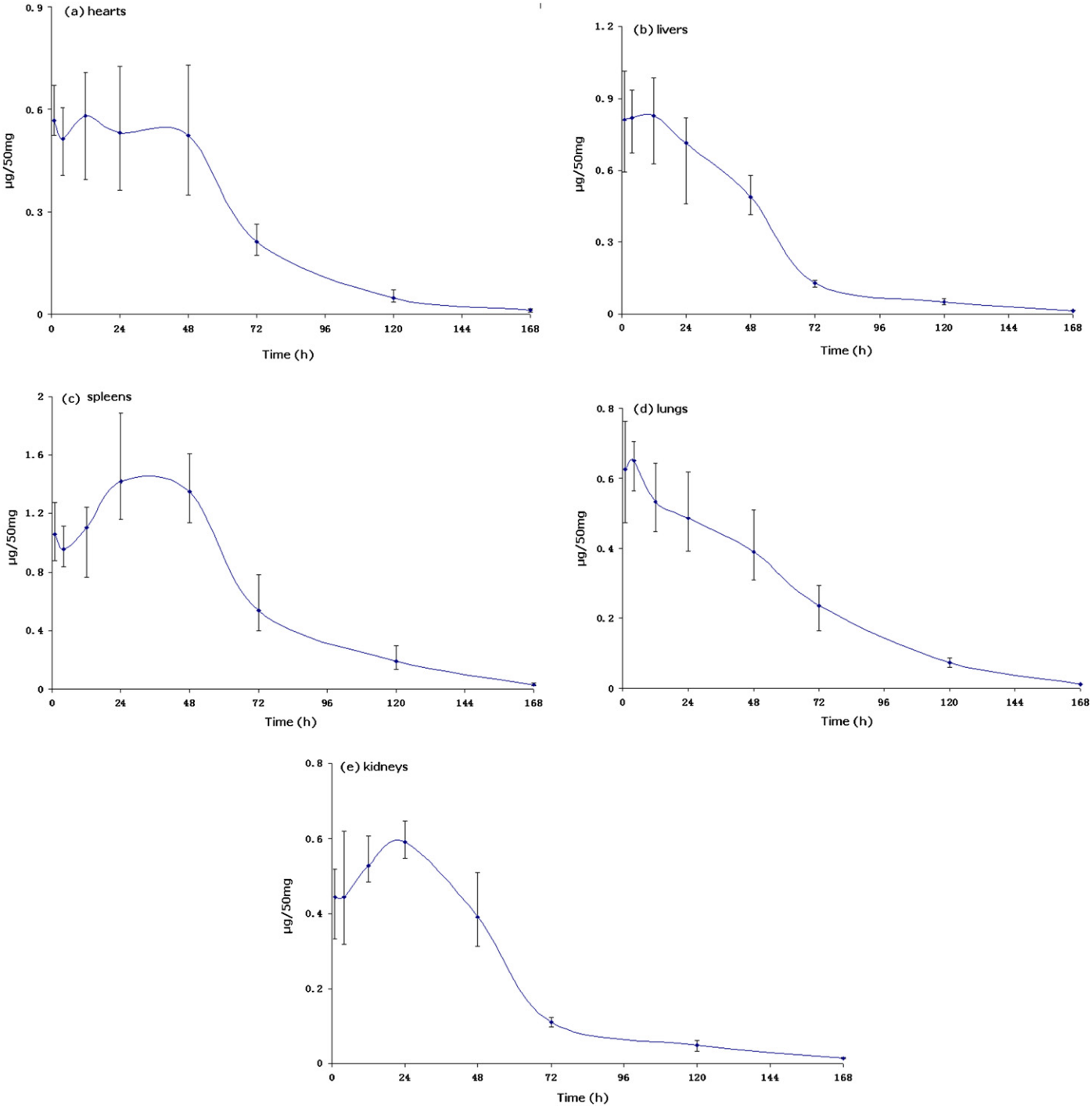

Fig. 5. Mean plasma concentration–time profile of 6 rats (a) hearts, (b) livers, (c) spleens, (d) lungs and (e) kidneys after intravenous administration of a single 5 mg kg^{-1} dose of DOXLI. The bars represent maximum absolute deviation values.

proportion and reached the maximum 71.2% with the ratio of PBS and methanol at 1:3 (v/v). However, the result was still unacceptable. Fortunately, our as-prepared magnetic MWNTs may be effective thermal generators, which could absorb NIR due to the MWNTs ingredients. Absorbed NIR promotes molecular oscillation leading to efficient heating of the surrounding environment, which can accelerate the DOX release speed from magnetic MWNTs. In order to investigate the effect of DOX desorption from magnetic MWNTs by NIR, the 808-nm continuous-wave NIR laser (power density, 10.4 W/cm^2; spot size, 6 mm × 8 mm; exposure duration, 5–20 s) was applied to illuminate the DOX-magnetic MWNTs with pH3.5 PBS:methanol (1:3, v/v) solution. Temperatures were measured by thermocouple. After a 10-s exposure to an 808 nm laser, the solution became warm and the temperature enhanced from 23 °C to 40 ± 0.3 °C. Varying NIR laser exposure time from 10 to 20 s led to a continuous rise of the thermal temperature. The recoveries of DOX were calculated to select the optimal NIR laser exposure time. Good recovery of 82.3% was obtained with 10 s of NIR laser exposure time, whereas the recoveries of 75.5% with 20 s. The result indicated that NIR illumination facilitated DOX release by 15.6% more than single extraction. However, when NIR laser exposure time remained longer than 20 s, agglomeration might emerge in

Table 2
Calibration, recovery and precision data of DOX. Different amounts of DOX and 10 μL of I.S. (200 μg/mL) were added to 50 mg of drug-free tissues samples to a final concentration of DOX at 0.005, 0.025, 0.05, 0.25, 0.5 and 1.25 μg/50 mg.

Matrix	Linear equation	R^2	Spiked level (μg/50 mg tissue)	Recovery (%)	Intra-day precision (RSD, %, $n = 3$)	Inter-day precision (RSD, %, $n = 3$)
Heart	$y = 0.5473x + 0.1117$	0.9941	0.005	81.2 ± 1.4	96.2 ± 1.8	92.8 ± 1.9
			0.05	84.5 ± 2.1	93.5 ± 1.7	91.5 ± 3.2
			1.25	82.6 ± 1.7	95.6 ± 0.9	91.6 ± 2.4
Liver	$y = 0.6704x + 0.0123$	0.9992	0.005	80.6 ± 1.8	94.1 ± 0.4	92.2 ± 3.8
			0.05	81.5 ± 1.5	94.8 ± 2.1	90.5 ± 1.3
			1.25	83.1 ± 0.6	95.7 ± 1.6	92.1 ± 2.9
Spleen	$y = 0.6678x - 0.0215$	0.9994	0.005	79.7 ± 1.2	95.8 ± 1.2	90.2 ± 0.8
			0.05	82.5 ± 2.6	93.2 ± 0.8	89.5 ± 1.7
			1.25	81.6 ± 2.1	95.3 ± 1.2	90.7 ± 2.8
Lung	$y = 0.6059x + 0.0415$	0.9976	0.005	84.2 ± 1.6	96.6 ± 0.4	92.2 ± 3.1
			0.05	80.8 ± 1.3	94.7 ± 2.9	88.3 ± 1.3
			1.25	82.1 ± 0.9	94.1 ± 1.5	90.7 ± 2.5
Kidney	$y = 0.6531x + 0.0242$	0.9983	0.005	79.5 ± 1.5	95.5 ± 0.9	89.0 ± 1.6
			0.05	80.2 ± 0.8	96.2 ± 1.6	92.0 ± 2.3
			1.25	83.7 ± 2.2	94.9 ± 2.0	90.9 ± 2.8

the magnetic MWNTs because of high solvent temperature (>50 °C) and thus reduce the recovery of DOX. Therefore, the optimized NIR illumination time of 10 s was selected.

3.4. Method validation

The results of calibrations were summarized in Table 2 with good linearity ($R^2 > 0.994$) for DOX in different tissues. The DL was 2 ng/50 mg tissue, which had enough sensitivity for the analysis of DOX in rat tissue samples in this study. The precision was determined by the percentage coefficient variation of within- and between-day variations at three different concentrations. The precision ranged from 93.2 to 96.6% for within-day measurement, and for between-day variation was in the range of 89.0–92.8%. These data disclosed that the described method had an accepted degree of precision. Recoveries were obtained from 79.5% to 84.2% by comparing the calculated content with the real values of the added DOX (Table 2). The results demonstrated that the suggested method was feasible for the analysis of DOX in rat tissue samples.

3.5. Determination of tissue distribution of DOXLI in rats

The present method was applied to the determination of tissue distribution of DOXLI in rats. Forty-eight male Kunming rats were given 5 mg kg^{-1} DOXLI via the jugular vein catheter. The analytical method was selective and had satisfactory separation of the target compounds with no interfering peaks in the chromatograms of drug-free tissues from healthy rats. The representative chromatograms of rat heart tissue after the injection of a single 5 mg kg^{-1} dose of DOXLI were depicted in Fig. 4. Using internal standard method, DOX concentrations in rat tissue samples collected at different times after administration were calculated and presented in Fig. 5a–e. The concentrations of DOX were highest in the spleen, followed by liver and lung, lowest in the heart and kidney. In addition, the pharmacokinetics of DOX in these organizations was also characteristic.

To demonstrate the proposed method, the approach of solvent extraction by chloroform:methanol (4:1, v/v) was also employed to analyze DOX in these samples. The DOX concentrations in rat tissue samples by solvent extraction were similar to those obtained by magnetic MWNTs extraction. The recoveries by solvent extraction were between 82.5% and 87.1%. However, solvent extraction is a time-consuming procedure and requires large amounts of organic solvents, which can cause harm to the human body and the surrounding environment. Comparatively, the method by magnetic MWNTs is more environment-friendly and is competent to DOX analysis in the field of tissue distribution.

4. Conclusion

In this study, magnetic MWNTs were successfully synthesized, and developed for the extraction and analysis of DOX in complex matrix of rat tissues. DOX could be greatly adsorbed via the π–π interaction between the aromatic ring(s) of the target analytes and the MWNTs. The DOX-magnetic MWNTs could be separated from the matrix solution easily owing to the magnetic Fe_3O_4 through a strong external magnetic field. The adsorbed analyte was easily desorbed with pH 3.5 PBS:methanol (1:3, v/v) solution combined with NIRAD technique. The as-prepared nanomaterial as sorbent was proved to provide good recoveries and precision for determination of tissue distribution of DOXLI in rats. Furthermore, we believe that this proposed method will be potentially useful for the analysis of other similar small molecular drugs in complex tissue or plasma samples.

Acknowledgement

This work was supported by the National Basic Research Program of China (973 Program, 2007CB935802).

Appendix A. Supplementary data

Supplementary data associated with this article can be found, in the online version, at doi:10.1016/j.chroma.2011.05.060.

References

[1] Z. Liu, K. Chen, C. Davis, S. Sherlock, Q.Z. Cao, X.Y. Chen, H.J. Dai, Cancer Res. 68 (2008) 6652.
[2] Z. Liu, S. Tabakman, K. Welsher, H.J. Dai, Nano Res. 2 (2009) 85.
[3] Z. Liu, X.M. Sun, N. Nakayama-Ratchford, H.J. Dai, ACS Nano 1 (2007) 50.
[4] A. Burkea, X.F. Dingb, R. Singha, R.A. Kraftb, N. Levi-Polyachenkoc, M.N. Rylanderd, C. Szotd, C. Buchanand, J. Whitneyd, J. Fisherd, H.C. Hatchera, R.D. Agostino, N.D. Kockg, P.M. Ajayanh, D.L. Carrollf, S. Akmana, F.M. Tortia, S.V. Torti, Proc. Natl. Acad. Sci. U.S.A. 106 (2009) 12897.
[5] M.L. Schipper, N.N. Ratchford, C.R. David, N.W.S. Kam, P. Chu, Z. Liu, X.M. Sun, H.J. Dai, S.S. Gambhir, Nat. Nanotechnol. 3 (2008) 216.
[6] J.W. Kim, E.I. Galanzha, E.V. Shashkov, H.M. Moon, V.P. Zharov, Nat. Nanotechnol. 4 (2009) 688.
[7] J.W. Fisher, S. Sarkar, C.F. Buchanan, C.S. Szot, J. Whitney, H.C. Hatcher, S.V. Torti, C.G. Rylander, M.N. Rylander, Cancer Res. 70 (2010) 9855.
[8] R.B. Li, R. Wu, L. Zhao, M.H. Wu, L. Yang, H.F. Zou, ACS Nano 4 (2010) 1399.
[9] H.K. Moon, S.H. Lee, H.C. Choi, ACS Nano 3 (2009) 3707.
[10] Z. Liu, A.C. Fan, K. Rakhra, S. Sherlock, A. Goodwin, X.Y. Chen, Q.W. Yang, D.W. Felsher, H.J. Dai, Angew. Chem., Int. Ed. 48 (2009) 7668.

[11] K. Pamornrat, T. Chongdee, T. Panote, K. Proespichaya, Microchem. J. 96 (2010) 317.
[12] Y.B. Lu, Q. Shen, Z.Y. Dai, H. Zhang, Anal. Bioanal. Chem. 398 (2010) 1819.
[13] A.S. Mohamed, B. Robert, Anal. Bioanal. Chem. 390 (2008) 2159.
[14] W.D. Wang, Y.M. Huang, W.Q. Shu, J. Cao, J. Chromatogr. A 1173 (2007) 27.
[15] W. Du, F.Q. Zhao, B.Z. Zeng, J. Chromatogr. A 1216 (2009) 3751.
[16] W.F. Chen, J.B. Zeng, J.M. Chen, X.L. Huang, Y.Q. Jiang, Y.R. Wang, X. Chen, J. Chromatogr. A 1216 (2009) 9143.
[17] H.H. See, M.M. Sanagi, W.A.W. Ibrahim, A.A. Naim, J. Chromatogr. A 1217 (2010) 1767.
[18] J.P. Ma, R.H. Xiao, J.H. Li, J.B. Yu, Y.Q. Zhang, L.X. Chen, J. Chromatogr. A 1217 (2010) 5462.
[19] L. Wang, J.M. Liu, P. Zhao, Z.W. Ning, H.L. Fan, J. Chromatogr. A 1217 (2010) 5741.
[20] M. Asensio-Ramos, J. Hernandez-Borges, T.M. Borges-Miquel, M.A. Rodriguez-Delgado, Anal. Chim. Acta 647 (2009) 167.
[21] Z. Guan, Y.M. Huang, W.D. Wang, Anal. Chim. Acta 627 (2008) 225.
[22] Q.X. Zhou, J.P. Xiao, Y.J. Ding, Anal. Chim. Acta 602 (2007) 223.
[23] M.A. Salam, R. Burk, J. Sep. Sci. 32 (2009) 1060.
[24] D.E. Mays, A. Hussam, Anal. Chim. Acta 646 (2009) 6.
[25] J.X. Wang, D.Q. Jiang, Z.Y. Gu, X.P. Yan, J. Chromatogr. A 1137 (2006) 8.
[26] H.X. Zhao, L.P. Wang, Y.M. Qiu, Z.Q. Zhou, W.K. Zhong, X. Li, Anal. Chim. Acta 586 (2007) 399.
[27] C.L. Chen, X.K. Wang, M. Nagatsu, Environ. Sci. Technol. 43 (2009) 2362.
[28] G.D. Chen, C.J. Alberts, W. Rodriguez, M. Toner, Anal. Chem. 82 (2010) 723.
[29] H.M. Chen, D.W. Qi, C.H. Deng, P.Y. Yang, X.M. Zhang, Proteomics 9 (2009) 380.
[30] H.M. Chen, X.Q. Xu, N. Yao, C.H. Deng, P.Y. Yang, X.M. Zhang, Proteomics 8 (2008) 2778.
[31] Y.F. Sha, C.H. Deng, B.Z. Liu, J. Chromatogr. A 1198–1199 (2008) 27.
[32] A. Ballesteros-Gomez, S. Rubio, Anal. Chem. 81 (2009) 9012.
[33] X.L. Zhang, H.Y. Niu, Y.Y. Pan, Y.L. Shi, Y.Q. Cai, Anal. Chem. 82 (2010) 2363.
[34] P.F. Yu, Q. Wang, X.F. Zhang, X.S. Zhang, S. Shen, Y. Wang, Anal. Chim. Acta 678 (2010) 50.
[35] G. Morales-Cid, A. Fekete, B.M. Simonet, R. Lehmann, S. Cardenas, X.M. Zhang, M. Valcarcel, P. Schmitt-Kopplin, Anal. Chem. 82 (2010) 2743.
[36] B.P. Jia, L. Gao, J. Sun, Carbon 45 (2007) 1476.
[37] X.H. Lu, H.Q. Liu, C.H. Deng, X.M. Yan, Chem. Commun. 47 (2011) 1210.
[38] Q. Lan, C. Liu, F. Yang, S.Y. Liu, J. Xu, D.J. Sun, J. Colloid Interface Sci. 310 (2007) 260.
[39] Y. Liu, W. Jiang, Y. Wang, X.J. Zhang, D. Song, F.S. Li, J. Magn. Magn. Mater. 321 (2009) 408.